Modeling miRNA-driven post-transcriptional regulation by using exon-intron split analysis (EISA) in pigs

Emilio Mármol-Sánchez[1*], Susanna Cirera[2], Laura M. Zingaretti[3], Mette Juul Jacobsen[2], Yuliaxis Ramayo-Caldas[4], Claus B. Jørgensen[2], Merete Fredholm[2], Tainã Figueiredo Cardoso[1†], Raquel Quintanilla[4], Marcel Amills[1,5]

[1]Centre for Research in Agricultural Genomics (CRAG), CSIC-IRTA-UAB-UB, Universitat Autònoma de Barcelona, 08193 Bellaterra, Spain.

[2]Department of Veterinary and Animal Sciences, Faculty of Health and Medical Sciences, University of Copenhagen, 1871 Frederiksberg C, Denmark.

[3]Universidad Nacional de Villa María, Villa María, Córdoba, Argentina.

[4]Animal Breeding and Genetics Program, Institute for Research and Technology in Food and Agriculture (IRTA), Torre Marimon, 08140 Caldes de Montbui, Barcelona, Spain.

[5]Departament de Ciència Animal i dels Aliments, Universitat Autònoma de Barcelona, 08193 Bellaterra, Barcelona, Spain.

*Emilio Mármol-Sánchez current address: Stockholm University, The Wenner-Gren Institute, Department of Molecular Biosciences, SciLifelab.

[†]Tainã Figueiredo Cardoso current address: Embrapa Pecuária Sudeste, Empresa Brasileira de Pesquisa Agropecuária (EMBRAPA), 13560-970, São Carlos, SP, Brazil.

Corresponding author: Emilio Mármol-Sánchez. Stockholm University, The Wenner-Gren Institute, Department of Molecular Biosciences, SciLifelab. Email: emilio.marmol.sanchez@gmail.com

Abstract

Bulk sequencing of RNA transcripts has typically been used to quantify gene expression levels in different experimental systems. However, linking differentially expressed (DE) mRNA transcripts to gene expression regulators, such as miRNAs, remains challenging, as miRNA-mRNA interactions are commonly identified *post hoc* after selecting sets of genes of interest, thus biasing the interpretation of underlying gene regulatory networks. In this study, we aimed at disentangling miRNA-driven post-transcriptional signals linked to porcine muscle and adipose tissue energy homeostasis. For this purpose, we performed an exon-intron split analysis (EISA) on muscle and fat RNA-seq data from two independent pig populations. One of these populations was subjected to fasting-feeding conditions, while the other represented divergent fatness profiles. After running EISA, protein-coding mRNA genes with downregulated exonic fractions and high post-transcriptional signals were significantly enriched for binding sites of DE upregulated miRNAs. Moreover, these downregulated genes showed an increased expression covariation for the exonic fraction compared to the intronic fraction. On the contrary, they did not show enrichment for binding sites of non-DE highly expressed or downregulated DE miRNAs. Among the set of loci displaying miRNA-driven post-transcriptional regulatory signals, we observed genes related to glucose homeostasis (*DKK2*, *PDK4*, *IL18*, *NR4A3*, *CHRNA1*, *TET2*), cell differentiation (*PBX1*, *BACH2*) and adipocytes metabolism (*SESN3*, *ESRRG*, *SAMD4*, *LEP*, *PTGFR*, *SERPINE2*, *RNF157*, *GPLD1*, *NCF2*, *OSBPL10*, *PRSS23*). Our results highlighted mRNA genes showing post-transcriptional miRNA-driven downregulation using the exonic and intronic fractions of RNA-seq datasets from muscle and adipose tissues in pigs.

Keywords: Exon-intron split analysis, microRNA, pigs, energy homeostasis.

1. Introduction

Messenger RNA (mRNA) expression and turnover in metabolic processes are subjected to complex yet poorly characterized regulatory mechanisms that contribute to shaping fine-tuned biological responses to different stimuli [1]. Cellular metabolic changes are hence a direct manifestation of intricate interactions between expressed transcripts and other regulatory elements that modify their abundance, localization, fate and degradation rate. MicroRNAs (miRNAs) are primarily engaged in the post-transcriptional control of gene expression through inhibition of translation and/or destabilization of target mRNAs by poly(A) shortening and subsequent degradation [2].

Changes in the abundance of mRNAs targeted by miRNAs can be inferred through covariation analysis. Such approach can help to unravel direct or indirect molecular interactions connecting and regulating biological networks.

In order to disentangle regulatory functions driven by miRNAs, research studies typically focus on specific sets of genes of interest, showing significant expression changes and harboring binding sites for DE miRNAs [3–9]. This approach, however, is biased by the fact that genes are selected after differential expression analysis and by the performance of an *ad hoc* search of predicted interactions between the 3'-UTRs of mRNAs and the seed regions of miRNAs. Besides, one of the main limitations of differential expression analysis is that it does not discriminate whether changes in expression take place either at the transcriptional or post-transcriptional levels. Such distinction is essential to understand at which level of the mRNA life-cycle the regulation is taking place.

To address this issue, Gaidatzis *et al*. [10] proposed that the magnitude of the post-transcriptional component can be deduced by comparing the amounts of exonic and intronic reads. Based on this, these authors devised a methodology denoted *exon-intron split analysis* (EISA), which separates the transcriptional and post-transcriptional

components of gene regulation. By considering that intronic reads are mainly derived from heterogeneous nuclear RNAs (unprocessed mRNAs or pre-mRNAs), they assessed the magnitude of the transcriptional regulation. Such assumption is based on early reports describing intronic expression as a proxy of nascent transcription and co-transcriptional splicing events [11–13]. In this way, a gene showing similar levels of intronic reads in two different states but a strong downregulation of exonic reads after applying a certain treatment or challenge (nutrition, infection, temperature etc.), could be indicative of an induced inhibition at the post-transcriptional level [10,14,15].

A high number of differential expression studies have been performed in pigs during the last decade [16–24], but to the best of our knowledge, in none of these studies the transcriptional and post-transcriptional components of gene regulation have been independently analyzed. In the present study, we aimed to dissect the contribution of miRNAs to post-transcriptional regulation in pigs by applying the EISA methodology using two independent porcine experimental models.

2. Materials and methods

2.1. Experimental design, sampling and processing

In this study, we have used two independent experimental systems:

(i) Duroc pigs: Twenty-three gilts divided in two fasting/feeding regimes, i.e., 11 gilts (*AL-T0*) slaughtered in fasting conditions and 12 gilts (*AL-T2*) slaughtered immediately after 7 h with access to *ad libitum* feed intake [7,22,25]. Immediately after slaughtering, *gluteus medius* (GM) skeletal muscle samples were collected and snap-frozen at -80°C.

(ii) Duroc-Göttingen minipig F_2 inter-cross: Ten individuals with divergent fatness profiles for their body mass index (BMI) metric (5 *lean* and 5 *obese*) were selected from

the UNIK resource population [26,27], as described in Jacobsen et al. 2019 [28]. Retroperitoneal adipose tissue was collected at slaughter and mature adipocytes were subsequently isolated following the protocol of Decaunes et al. 2011 [29] with modifications reported in [28].

Further details about RNA-seq and small RNA-seq expression data generated from both experimental designs have been previously described [7,22,28]. Sequencing reads generated in the RNA-Seq and small RNA-Seq datasets from both pig resources were trimmed with the Cutadapt software [30]. Reads were mapped against the Sscrofa11.1 porcine assembly [31] with the HISAT2 aligner [32] and default parameters for RNA-Seq reads. In contrast, the Bowtie Alignment v.1.2.1.1 software [33] with small sequence reads specifications (*bowtie -n 0 -l 25 -m 20 -k 1 --best --strata*) was used to align small RNA-Seq reads to the Sscrofa11.1 porcine reference assembly [31].

2.2. Exon/Intron quantification

We generated exonic and intronic-specific annotations spanning all genes available using the gtf formatted Sscrofa.11.1 v.103 gene annotation file (Ensembl repositories: http://ftp.ensembl.org/pub/release-103/gtf/sus_scrofa/). Overlapping intronic/exonic regions, as well as singleton positions were removed [34]. Each intronic region was trimmed by removing 10 nucleotides on both ends to avoid exonic reads mapping close to exon/intron junctions. We then used the featureCounts function included in the Rsubread package [35] to quantify gene expression profiles based on exonic and intron expression patterns for each gene, independently. MiRNA expression profiles were estimated using the Sscrofa11.1 v.103 mature miRNA annotation with the featureCounts software tool [36] in single-end mode and with default parameters.

126 **2.3. Exon/intron split analysis (EISA).**

127 We applied EISA to infer post-transcriptional gene regulation in our two independent
128 porcine datasets. For this purpose, we separately estimated the exonic and intronic
129 abundance of each annotated mRNA gene using the Sscrofa11.1 v.103 exon/intron
130 custom annotation generated as described above. Only genes showing average expression
131 values above 1 count-per-million in at least 50% of animals were retained for further
132 analyses. Normalization was performed independently for exon and intron counts by
133 multiplying each i^{th} gene expression in each j^{th} sample by the corresponding mean gene
134 expression and dividing by the total number of quantified counts per sample [10]. Exonic
135 and intronic gene abundances were subsequently transformed to a $\log_2$ scale, adding a
136 pseudo-count of 1 and averaged within each considered treatment groups (*AL-T0* and *AL-*
137 *T2* for GM tissues and *lean* and *obese* for adipocyte isolates).
138 Only genes with successful exonic and intronic quantified read counts were considered
139 in our analyses. The transcriptional component (Tc) contribution to the observed
140 differences in each i^{th} gene was expressed as the increment of intronic counts in fed (*AL-*
141 *T2*) and *obese* animals with respect to fasting (*AL-T0*) and *lean* animals ($\Delta Int = Int_{2i} -$
142 Int_{1i}), respectively. The increment of exonic counts (ΔEx) was also calculated, and the
143 post-transcriptional component (PTc) effect was expressed as $\Delta Ex - \Delta Int = (Ex_{2i} - Ex_{1i})$
144 $- (Int_{2i} - Int_{1i})$. Both components were z-scored to represent comparable ranges between
145 ΔEx and ΔInt estimates. All implemented analyses have been summarized in **Fig. S1**. A
146 ready-to-use modular pipeline for running EISA is publicly available at
147 https://github.com/emarmolsanchez/EISACompR
148

149 **2.4. Post-transcriptional signal prioritization**

In order to obtain a prioritized list of genes showing relevant signals of post-transcriptional regulation, the top 5% genes with the highest negative PTc scores were retrieved. We only focused on genes showing strongly reduced exonic fraction (ΔEx) values of at least 2-folds for post-transcriptional signals in both experimental systems.

2.5. Differential expression analyses and significance of PTc scores

Differential expression analyses were carried out with the *edgeR* package [37] by considering the exonic fraction of mRNAs, as well as miRNA expression profiles from RNA-Seq and small RNA-Seq datasets, respectively, and in the two experimental systems under study. Expression filtered raw counts for exonic reads were normalized with the trimmed mean of M-values normalization (TMM) method [38] and the statistical significance of mean expression differences was tested with a quasi-likelihood F-test [37]. Correction for multiple hypothesis testing was implemented with the Benjamini-Hochberg false discovery rate approach [39]. Messenger RNAs were considered as differentially expressed (DE) when the absolute value of the fold-change (FC) was higher than 2 ($|FC| > 2$) and q-value < 0.05. For miRNAs, $|FC| > 1.5$ and q-value < 0.05 were used instead. This more flexible threshold was motivated by the fact that miRNAs are commonly lowly expressed and show more stable and subtle expression changes compared to mRNAs [7,40]. The statistical significance of the post-transcriptional (PTc) scores was evaluated by incorporating the intronic quantification as an interaction effect for exonic abundances [10]. The fasting pigs (*AL-T0*) from Duroc skeletal muscle, as well as *obese* pigs from Duroc-Göttingen adipocyte expression profiles were considered to be the baseline controls, i.e., any given upregulation in ΔEx or ΔInt values represents and overexpression in fed (*AL-T2*) Duroc gilts and *lean* Duroc-Göttingen minipigs with respect to their fasting (*AL-T0*) and *obese* counterparts.

175

176 **2.6. miRNA target prediction**

177 Putative interactions between the seed regions of expressed miRNAs (small RNA-seq
178 datasets) and the 3'-UTRs of expressed protein-coding mRNA genes (RNA-seq datasets)
179 were predicted on the basis of sequence identity using the Sscrofa11.1 reference
180 assembly. The annotated 3'-UTRs longer than 30 nts from porcine mRNAs were retrieved
181 from the Sscrofa11.1 v.103 available at BioMart (http://www.ensembl.org/biomart) and
182 miRBase [41] databases. Redundant seeds from mature porcine microRNAs were
183 removed. The seedVicious v1.1 tool [42] was used to infer miRNA-mRNA interactions.
184 MiRNA-mRNA 8mer, 7mer-m8 and 7mer-A1 interactions were considered as the most
185 relevant among the full set of canonical and non-canonical interactions [2,43,44].
186 Based on the study of Grimson et al. [43], the *in silico*-predicted miRNA-mRNA
187 interactions matching any of the following criteria were removed: (i) Binding sites located
188 in 3'-UTRs at less than 15 nts close to the end of the open reading frame (and the stop
189 codon) or less than 15 nts close to the terminal poly(A) tail (E criterion), (ii) binding sites
190 located in the middle of the 3'-UTR in a range comprising 45-55% of the central region
191 of the non-coding sequence (M criterion), and (iii) binding sites lack AU-rich elements
192 in their immediate upstream and downstream flanking regions comprising 30 nts each
193 (AU criterion).
194 Covariation patterns between miRNAs and their predicted mRNA targets were assessed
195 by computing Spearman's correlation coefficients (ρ) with the TMM normalized and $\log_2$
196 transformed expression profiles of the exonic fractions of mRNA and miRNA genes. To
197 determine the contribution of miRNAs to post-transcriptional regulation in the two
198 experimental systems under study, only miRNA-mRNA predicted pairs comprising DE
199 upregulated miRNAs (FC > 1.5; q-value < 0.05) and mRNA genes with relevant PTc

scores (see post-transcriptional signal prioritization section) were taken into consideration.

2.7. miRNA target enrichment analyses

We sought to determine if the overall number of mRNA genes with high post-transcriptional signals (the ones with the top 5% negative PTc scores and reduced ΔEx values > 2-folds) were significantly enriched to be targeted by at least one upregulated miRNA (FC > 1.5; *q*-value < 0.05), compared with the whole set of expressed mRNAs genes with available 3'-UTRs from both datasets. Enrichment analyses were carried out using the Fisher's exact test implemented in the *fisher.test* R function. Significance level was set at nominal *P*-value < 0.05.

We also tested whether these genes were enriched for binding sites of the top 5% most highly expressed miRNA genes, excluding significantly upregulated miRNAs, as well as for binding sites of significantly downregulated miRNAs (FC < -1.5; *q*-value < 0.05). Given the relatively low statistical significance of DE miRNAs observed in the UNIK Duroc-Göttingen minipigs (l*ean* vs *obese*), we considered that miRNAs were significantly upregulated in this particular data set when FC >1.5 and *P*-value < 0.01.

As a control randomized test for enrichment analyses between miRNAs and mRNAs with high post-transcriptional downregulatory signals, we implemented a bootstrap corrected iteration to generate 100 random sets of 10 expressed mature miRNA genes without seed redundancy, which were used as input for miRNA target prediction with the sets of mRNA genes with the high post-transcriptional signals (top 5% PTc scores and at least 2-folds ΔEx reduction). The distribution of odds ratios obtained after iterating over each random set of miRNAs (N = 100) were then compared with odds ratios obtained with the set of significantly upregulated miRNAs.

The *P*-value for the significance of the deviation of observed odds ratios against the bootstrapped odds ratios distribution was defined as, $P - value = 1 - \frac{r+1}{k+1}$, where r is the number of permuted odds ratios with values equal or higher than the observed odds ratio for enrichment analyses with the set of upregulated miRNAs, and k is the number of defined permutations (N = 100).

2.8. Gene covariation network and covariation enrichment score

We computed pairwise correlation coefficients among the whole set of DE mRNA genes in the *AL-T0* vs *AL-T2* (q-value < 0.05, N = 454) and *lean* vs *obese* (q-value < 0.05, N = 299). These correlations were compared with those corresponding to the set of genes with relevant post-transcriptional signals and putatively targeted by DE upregulated miRNAs. Normalized exonic and intronic estimates in the $\log_2$ scale obtained from EISA analyses were used to compute Spearman's correlation coefficients (ρ) for each potential pair of DE mRNA genes plus those with post-transcriptional signals but without significant DE. Self-correlation pairs were excluded. Significant correlations were identified with the Partial Correlation with Information Theory (PCIT) network inference algorithm [45] implemented in the *pcit* R package [46]. Non-significant covarying pairs were set to zero, while a value of 1 was assigned to the significant ones with both positive or negative coefficients $|\rho| > 0.6$.

The potential contribution of miRNAs to shape the observed covariation patterns was assessed by calculating a covariation enrichment score (CES) following Tarbier et al. 2020 [47]. If multiple genes are downregulated by any upregulated miRNAs in a coordinated manner, we would expect to observe a reduced abundance in their mature spliced mRNA forms but not in the corresponding primary transcripts, i.e., we would detect a covariation only for the exonic fractions (but not for the intronic ones). In other

words, the intronic fraction, eventually spliced and degraded in the nucleus, should not reflect any posterior post-transcriptional regulatory effects in the cytoplasm, so little or null covariation might be expected. Significant differences among the set of exonic, intronic and control CES values were tested with a non-parametric approach using a Mann-Whitney U non-parametric test [48]. Further details can be found in **Supplementary Methods**.

2.9. Estimating the expression levels of miRNAs and several of their predicted mRNA targets by qPCR

The same total RNA extracted from adipocytes and used for sequencing was subsequently employed for cDNA synthesis and qPCR verification. Five mRNAs (*LEP*, *OSBLP10*, *PRSS23*, *RNF157* and *SERPINE2*) among the top 5% negative PTc scores and showing at least 2-folds reduction in their ΔEx values were selected for qPCR profiling. Two reference genes (*TBP* and *ACTB*, as defined by Nygard et al. 2007 [49]) were used for normalization. Accordingly, three of the most DE miRNAs were selected for qPCR profiling (ssc-miR-92b-3p, ssc-miR-148a-3p and ssc-miR-214-3p), plus two highly expressed non-DE miRNAs for normalization (ssc-let-7a and ssc-miR-23a-3p) from the *lean* vs *obese* small RNA-Seq dataset. Further details about qPCR experimental procedures are available in **Supplementary Methods**. All primers for mRNA and miRNA expression profiling are available at **Table S2**. Raw Cq values for each assay are available at **Table S3**.

3. Results

3.1. The analysis of post-transcriptional regulation in muscle samples from fasting and fed Duroc gilts

Identification of genes predicted to be post-transcriptionally regulated by miRNAs

After the processing, mapping and quantification of mRNA and miRNA expression levels in GM skeletal muscle samples from Duroc gilts, an average of 45.2 million reads per sample (~93%) were successfully mapped to 31,908 genes annotated in the Sscrofa11.1 v.103 assembly (including protein coding and non-coding genes). Besides, an average of 2.2 million reads per sample (~42%) mapped to 370 annotated porcine miRNA genes.

A total of 30,322 (based on exonic reads) and 22,769 (based on intronic reads) genes were successfully quantified after splitting the reference Sscrofa11.1 v.103 assembly between exonic and intronic features. The exonic fraction displayed an average of 1,923.94 estimated counts per gene, whereas the intronic fraction showed an average of 83.02 counts per gene. In other words, exonic counts were ~23 fold more abundant than those corresponding to intronic regions.

Differential expression analyses based on exonic fractions identified 454 DE genes. Among those, only genes with |FC| > 2 were retained, making a total of 52 upregulated and 80 downregulated genes in the *AL-T0* vs *AL-T2* comparison (**Table S4, Fig. S2A**). Besides, differential expression analyses on small RNA-seq data revealed 16 DE miRNAs, of which 8 were upregulated in *AL-T2* pigs, representing 6 unique miRNA seeds (**Table S5**). These non-redundant seeds of significantly upregulated miRNAs in fed animals (ssc-miR-148a-3p, ssc-miR-7-5p, ssc-miR-30-3p, ssc-miR-151-3p, ssc-miR-374a-3p and ssc-miR-421-5p) were selected as potential post-transcriptional regulators of GM muscle mRNA expression in response to nutrient supply. EISA results made possible to detect 133 genes with significant effects (**Table S6**), of which three had > 2-

298 folds reduced ΔEx fractions and two of them had significantly negative PTc scores (**Table**
299 **1**).

300 To detect mRNA genes putatively downregulated by miRNAs at the post-transcriptional
301 level, mRNA genes displaying the top 5% negative PTc scores with at least 2-folds ΔEx
302 reduction were selected as putative miRNA-targets (**Fig. S2B**). With this approach, 26
303 mRNA genes were selected (**Table 1**). One of them (ENSSSCG00000049158) did not
304 have a properly annotated 3´-UTR so it was excluded from further analyses. Among this
305 set of genes with high post-transcriptional signals, 18 appeared as significantly
306 downregulated (FC < -2; *q*-value < 0.05) in the differential expression analysis
307 considering their exonic fractions (**Table 1** and **Table S4**).

308

309

310 **Table 1:** mRNA genes with the top 5% post-transcriptional (PTc) scores and at least 2-
311 folds exonic fraction (ΔEx) reduction (equivalent to -1 in the $\log_2$ scale) from *gluteus*
312 *medius* skeletal muscle expression profiles of fasting (*AL-T0*, N = 11) and fed (*AL-T2*, N
313 = 12) Duroc gilts.

ID	Gene	$\log_2$FC	ΔEx	PT_c	*P*-value	*q*-value	DE	miRNA target
ENSSSCG00000032094	*DKK2*	-2.010	-1.431	-4.738	1.654E-05	3.830E-03	•	x
ENSSSCG00000015334	*PDK4*	-2.108	-5.250	-4.698	4.693E-03	1.330E-01	x	x
ENSSSCG00000015037	*IL18*	-1.655	-1.191	-3.682	4.787E-03	1.340E-01	•	x
ENSSSCG00000005385	*NR4A3*	-1.337	-3.082	-3.646	4.038E-02	4.098E-01	x	x
ENSSSCG00000003766	*DNAJB4*	-1.391	-1.008	-3.348	8.358E-03	1.905E-01		x
ENSSSCG00000015969	*CHRNA1*	-1.561	-1.339	-3.341	2.606E-03	9.406E-02	x	x
ENSSSCG00000039419	*SLCO4A1*	-1.055	-2.279	-3.180	2.820E-02	3.544E-01	x	x
ENSSSCG00000049158		-1.107	-1.096	-3.164	3.182E-02	3.735E-01		x
ENSSSCG00000004347	*FBXL4*	-1.298	-1.126	-3.133	1.422E-03	6.520E-02	x	x
ENSSSCG00000004979	*MYO9A*	-1.239	-1.003	-3.043	7.296E-03	1.731E-01		x
ENSSSCG00000013351	*NAV2*	-1.163	-1.196	-2.863	2.605E-04	2.301E-02	x	x
ENSSSCG00000032741	*TBC1D9*	-0.913	-1.061	-2.736	1.534E-02	2.583E-01	•	x
ENSSSCG00000031728	*ABRA*	-1.238	-1.393	-2.704	1.295E-03	6.116E-02	x	x
ENSSSCG00000006331	*PBX1*	-0.891	-1.039	-2.480	1.135E-02	2.177E-01	x	x
ENSSSCG00000035037	*SIK1*	-1.357	-1.289	-2.475	3.999E-03	1.212E-01	x	x
ENSSSCG00000038374	*CIART*	-1.027	-1.321	-2.052	1.543E-02	2.587E-01	x	

ENSSSCG00000023806	*LRRN1*	-0.776	-1.013	-1.983	1.580E-01	7.074E-01		x
ENSSSCG00000009157	*TET2*	-0.381	-1.123	-1.792	4.880E-01	9.582E-01		x
ENSSSCG00000011133	*PFKFB3*	-0.022	-2.256	-1.785	9.712E-01	9.987E-01	x	x
ENSSSCG00000002283	*FUT8*	-0.578	-1.286	-1.784	9.887E-02	6.059E-01	x	x
ENSSSCG00000023133	*OSBPL6*	-0.432	-1.088	-1.772	3.835E-01	9.108E-01	x	
ENSSSCG00000017986	*NDEL1*	-0.767	-1.644	-1.759	1.006E-02	2.081E-01	x	x
ENSSSCG00000031321	*NR4A1*	-0.630	-1.328	-1.720	6.298E-02	5.006E-01	x	
ENSSSCG00000035101	*KLF5*	-0.519	-1.487	-1.708	2.942E-01	8.488E-01	x	x
ENSSSCG00000004332	*BACH2*	-0.714	-2.105	-1.705	9.089E-02	5.861E-01	x	x
ENSSSCG00000017983	*PER1*	-0.773	-1.073	-1.627	3.000E-02	3.662E-01	x	

[a]Log_2FC: estimated log_2 fold change for mean exonic fractions from *gluteus medius* expression profiles of fasted *AL-T0* and fed *AL-T2* Duroc gilts; [b]ΔEx: exonic fraction increment ($Ex_2 – Ex_1$) when comparing exon abundances in *AL-T0* (Ex_1) vs *AL-T2* (Ex_2) Duroc gilts; [c]PTc: post-transcriptional signal (ΔEx – ΔInt) in z-score scale; [d]q-value: q-value calculated with the false discovery rate (FDR) approach [39]. The "x" symbols represent differentially expressed (DE) genes (FC < -2; *q*-value < 0.05) according to their exonic fractions, as well as those targeted by at least one of the upregulated miRNAs excluding redundant seeds (N = 6, **Table S5**). The "•" symbol represents suggestive differential expression (*P*-value < 0.01, **Table S4**).

Context-based pruning of predicted miRNA-mRNA interactions removes spurious unreliable target events

As a first step to determine if genes with highly negative PTc scores and showing a marked reduction in exonic fractions were repressed by upregulated DE miRNAs (**Table S5**), we investigated the accuracy and reliability of *in silico* predictions regarding miRNA binding sites in their 3'-UTRs (**Table S7**). We evaluated the presence of enriched binding sites over a random background of expressed genes with no context-based removal of predicted binding sites, applying each one of the three selection criteria reported in Methods independently, as well as by combining them pairwise or altogether. As depicted in **Fig. S3A** and **S3B**, introducing additional context-based filtering criteria for removing spurious unreliable binding site predictions resulted in an overall increased enrichment of miRNA targeted genes within the top 1% (**Fig. S3A**) and 5% (**Fig. S3B**) negative PTc

scores and displaying > 2-folds ΔEx reduction. This significantly increased enrichment was more evident when using the AU criterion, as shown in **Fig. S3A**. However, we also detected a slight increment when adding the other two context-based removal criteria (M and E). These findings were less evident when taking into consideration the list of the top 5% genes (**Fig. S3B**). Nevertheless, an increased enrichment for targeted mRNAs by DE upregulated miRNAs was detectable for all combined filtering criteria, especially for 7mer-A1 binding sites, and probably at the expense of the scarcer and more efficient 8mer binding sites. Based on these results, we decided to apply the three joint criteria (AU, M and E) for enrichment analyses between the set of mRNA genes with high post-transcriptional signals and putatively targeted by miRNAs.

Genes with relevant post-transcriptional signals are enriched for putative miRNA binding sites in their 3'-UTRs

Target prediction and context-based pruning of miRNA-mRNA interactions for mRNA genes displaying the top 5% negative PTc scores and at least 2-folds reductions in the ΔEx exonic fraction (N = 25 after excluding ENSSSCG00000049158; **Fig. 1A**) made possible to detect 11 8mer, 21 7mer-m8 and 22 7mer-A1 miRNA binding sites (**Table S7**) corresponding to the 6 non-redundant seeds of DE miRNAs upregulated in *AL-T2* gilts. This set of 25 mRNA genes showing putative post-transcriptional repression by miRNAs showed a significant enrichment in 8mer, 7mer-m8 and 7mer-A1 sites (**Fig. 1B**), and this was especially relevant when combining these three types of binding sites. More importantly, 21 out of these 25 genes were predicted as putative targets of miRNAs upregulated in the GM muscle samples from *AL-T2* fed gilts (**Table 1** and **Table S5**).

We also evaluated the enrichment of the mRNA genes with the top 5% negative PTc scores and at least 2-folds ΔEx reduction (N = 25, **Table 1**) to be targeted by the following

sets of miRNAs: (i) Non-redundant miRNAs downregulated in *AL-T2* fed gilts (ssc-miR-1285, ssc-miR-758, ssc-miR-339, sc-miR-22-3p, ssc-miR-296-5p, ssc-miR-129a-3p, ssc-miR-181c and ssc-miR-19b, **Table S5**), (ii) the top 5% most expressed miRNAs, excluding those being upregulated (ssc-miR-1, ssc-miR-133a-3p, ssc-miR-26a, ssc-miR-10b, ssc-miR-378, ssc-miR-99a-5p, ssc-miR-27b-3p, ssc-miR-30d, ssc-miR-486 and ssc-let-7f-5p), and (iii) for an iteration (N = 100) of random sets of 10 expressed miRNAs, irrespective of their DE and abundance status, as a control test. None of these additional analyses recovered a significant enrichment for any type of the three considered miRNA target subtypes (**Fig. 1B**).

The mRNA with the highest and significant PTc score was the Dickkopf WNT Signaling Pathway Inhibitor 2 (*DKK2*), and thus, this was the gene with the highest putative miRNA-driven downregulation and no additional transcriptional influence (**Table 1**). Moreover, the DKK2 locus was the only gene harboring two miRNA 8mer binding sites (**Table S7**), although it was not among the most highly DE mRNA genes according to differential expression analyses (**Table S4**). As depicted in **Table 1**, only suggestive significant differences (*P*-value < 0.01) in mean expression were found for *DKK2* transcripts. Besides, among the set of mRNA genes displaying the top 5% PTc scores and at least 2-folds ΔEx reduction (**Table 1**), 5 were not DE, and 3 of them only showed suggestive DE, while the rest of DE mRNAs displayed a wide range of significance (**Table S4**). The divergence between EISA and differential expression results is also shown in **Fig. 1C**, where not all the mRNA genes highlighted by EISA (**Fig. 1A**) were DE downregulated loci.

The miRNAs with the highest number of significant miRNA-mRNA interactions (in terms of correlations between their expression levels) were ssc-miR-30a-3p and ssc-miR-421-5p, which showed 9 and 8 significant miRNA-mRNA interactions, followed by ssc-

386 miR-148-3p with 4 significant interactions with mRNA genes showing significant post-
387 transcriptional signals (**Table S7**).
388
389 *Genes showing post-transcriptional regulatory signals predominantly covary at the*
390 *exonic level*
391 To further elucidate whether genes displaying the top 5% PTc scores are strong candidates
392 to be regulated by miRNAs according to *in silico* predictions (N = 21), we evaluated the
393 covariation patterns among them and with the whole set of 454 mRNA genes DE between
394 *AL-T0* and *AL-T2* gilts.
395 By calculating CES values (see Methods) for the 21 genes putatively targeted by DE
396 upregulated miRNAs, we obtained an estimation of the fold change in their observed
397 covariation with respect to other 435 DE mRNAs. CEs values were measured for both
398 their exonic and intronic fractions. Our analyses revealed that 19 out of these 21 genes
399 showed an increased covariation of approximately 2-folds in their exonic fractions when
400 compared to their intronic fractions (**Table S8**, **Fig. 1D**). When we iteratively analyzed
401 the observed fold change in covariation for random sets of genes (N = 1,000), they
402 displayed CES ≈ 1, indicative of no covariation (**Fig. 1D**). The observed CES
403 distributions of exonic, intronic and control sets were significantly different (*P*-value =
404 3.663E-06) after running non-parametric tests (**Fig. 1D**), thus supporting that the genes
405 displaying the top 5% PTc scores are probably repressed by DE upregulated miRNAs.
406
407

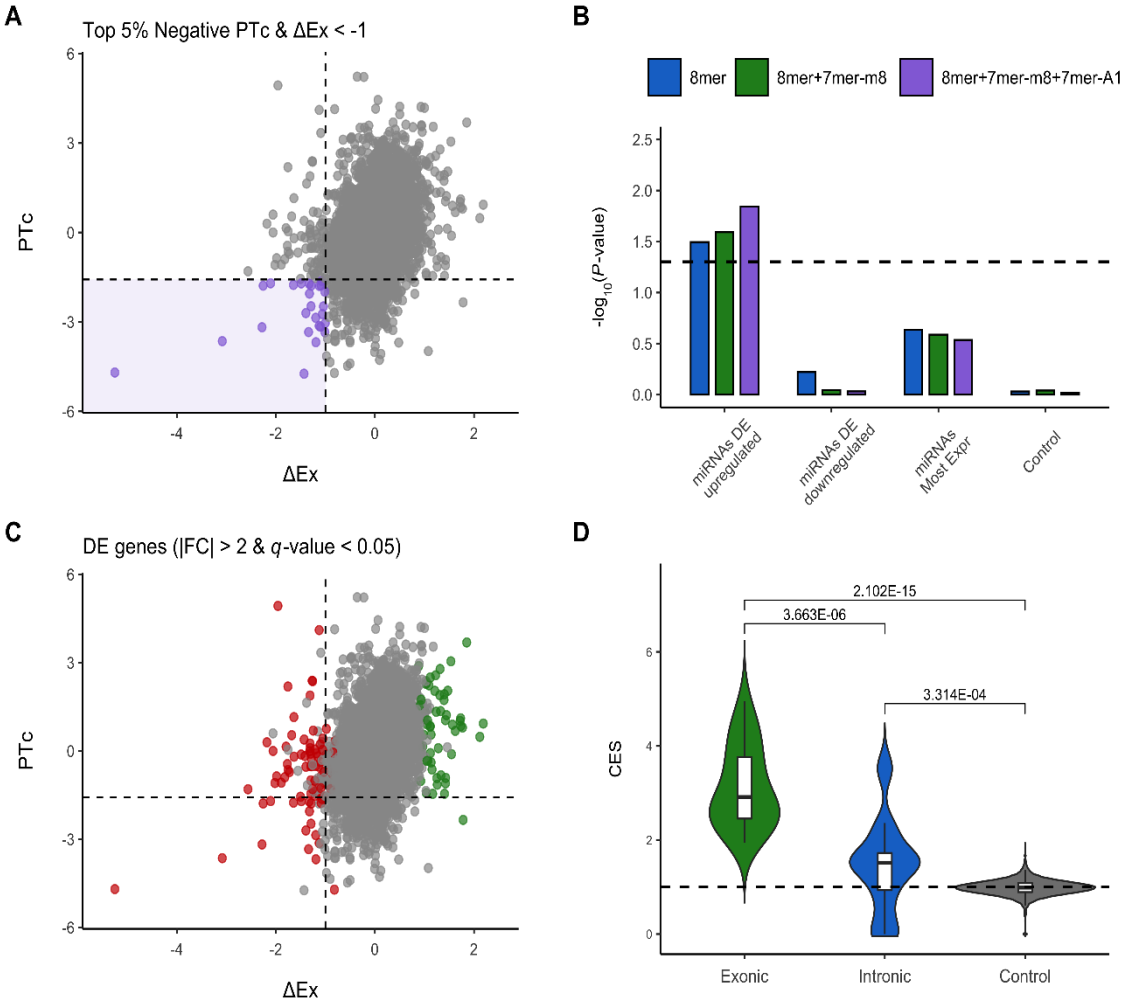

408

409

410 **Figure 1:** (**A**) Scatterplot depicting mRNA genes with the top 5% negative PTc scores
411 and at least 2-folds ΔEx reduction according to exonic (ΔEx) and PTc (ΔEx – ΔInt) values
412 (in purple) and putatively targeted by DE upregulated miRNAs (FC > 1.5; *q*-value < 0.05)
413 from *gluteus medius* skeletal muscle expression profiles of fasted (*AL-T0*, N = 11) and
414 fed (*AL-T2*, N = 12) Duroc gilts. (**B**) Enrichment analyses of the number of mRNA genes
415 with the top 5% negative PTc scores and at least 2-folds ΔEx reduction putatively targeted
416 by DE upregulated miRNAs (FC > 1.5; *q*-value < 0.05), DE downregulated miRNAs (FC
417 < -1.5; *q*-value < 0.05) and the top 5% most highly expressed miRNAs, excluding DE
418 upregulated miRNAs. (**C**) Scatterplot depicting DE upregulated (in green) and
419 downregulated (in red) mRNA genes (|FC| > 2; *q*-value < 0.05) according to exonic (ΔEx)

and PTc (ΔEx – ΔInt) values. (**D**) Covariation enrichment scores (CES) for the exonic and intronic fractions of mRNA genes with the top 5% negative PTc scores and at least 2-folds ΔEx reduction, putatively targeted by upregulated miRNAs from *gluteus medius* skeletal muscle expression profiles of fasted (*AL-T0*, N = 11) and fed (*AL-T2*, N = 12) Duroc gilts. The control set of CES values were generated by permuted (N = 1,000) random sets of exonic and intronic profiles of genes with the same size as those used before (N = 21). Significant differences were assessed using a Mann-Whitney U non-parametric test [48].

3.2. Studying post-transcriptional signals in fat metabolism using an independent Duroc-Göttingen minipig population

After pre-processing and filtering of sequenced reads from adipocytes samples, we were able to retrieve ~98.1 and ~0.87 million mRNA and small RNA reads per sample, and ~96.5% and ~73.4% of these reads mapped to annotated porcine mRNA and miRNA genes, respectively. Differential expression analyses revealed a total of 299 DE mRNAs, of which 52 were downregulated and 95 were upregulated, respectively (**Table S9**). Regarding miRNAs, only one gene (ssc-miR-92b-3p) was significantly upregulated in *lean* pigs, while 7 additional miRNAs showed suggestive differential expression (*P*-value < 0.01), of which 4 were downregulated, and one (ssc-miR-92a) had the same seed sequence as ssc-miR-92b-3p (**Table S10**).

After running EISA on the mRNA expression profiles for exonic and intronic fractions, a total of 44 downregulated mRNAs in *lean* pigs displayed the top 5% PTc scores with reduced ΔEx > 2-folds (**Table S11, Fig. 2A**). One of them (ENSSSCG00000016928) did not have a properly annotated 3´-UTR so it was excluded from further analyses. The

whole set of mRNA genes from EISA results is available at **Table S12**. Among this set of genes with high post-transcriptional signals, 13 appeared as significantly downregulated (FC < -2; *q*-value < 0.05) and 9 had suggestive repression (*P*-value < 0.01) in the differential expression analysis considering their exonic fractions (**Table S9** and **S11**). In this dataset, the sestrin 3 (*SESN3*) locus showed the second highest negative PTc score, but was the only one among the rest of highlighted genes where a significant post-transcriptional signal was observed (**Table S11**), i.e., equivalent to the *DKK2* gene in Duroc pigs, this was the only locus showing post-transcriptional regulation with no additional co-occurring transcriptional signal. Such strong downregulation was also evidenced in differential expression analyses, where it was the most significantly DE gene (**Table S9**).

From the set of downregulated genes, 25 out of the 43 mRNA genes analyzed for miRNA binding sites were classified as putative targets of the set of miRNAs upregulated in *lean* pigs (ssc-miR-92b-3p, ssc-miR-148a-3p, ssc-miR-204 and ssc-miR-214-3p; **Table S10**). Target prediction and context-based pruning of miRNA-mRNA interactions for these 43 mRNA genes made it possible to detect 8 8mer, 21 7mer-m8 and 24 7mer-A1 miRNA binding sites (**Table S13**) corresponding to the non-redundant seeds of selected upregulated miRNAs (N = 4) in *lean* minipigs (**Table S10**). The *SESN3* gene showed the highest number of predicted putative miRNA target sites in its 3´-UTR (**Table S13**).

Enrichment analyses for the set of putative miRNA target genes with the top 5% negative PTc scores and at least 2-folds ΔEx reduction (N = 25, **Table S11**) revealed no significant enrichment for the three types of miRNA target sites considered, although a slight increase when considering 8mer + 7mer-m8 binding sites and all three types together could be observed (**Fig. 2B**). Among this set of 25 genes, 7 appeared as significantly downregulated (FC < -2; *q*-value < 0.05) and 6 had suggestive repression (*P*-value < 0.01)

in the differential expression analysis considering their exonic fractions (**Table S9** and **S11**, **Fig. 2C**).

In agreement with results obtained for the first studied skeletal muscle expression dataset, the exonic fraction of the mRNA genes putatively targeted by upregulated miRNAs in lean pigs showed approximately 2-folds significantly increased covariation (*P*-value = 2.703E-02) with regard to their intronic fraction (**Fig. 2D**). Besides, 18 out of these 25 mRNA genes showed an overall increased covariation in their exonic fractions compared with their intronic fractions, expressed as the increment in their CES values (ΔCES = exonic CES – intronic CES, **Table S14**).

Because adipose tissue samples were available, qPCR analyses were performed to assess whether mRNAs among the top 5% negative PTc scores and with at least 2-folds ΔEx reduction together with upregulated miRNAs displayed patterns of expression consistent with those obtained in the RNA-seq and small RNA-seq experiments. To this end, we selected five mRNAs (*LEP*, *OSBPL10*, *PRSS23*, *RNF157* and *SERPINE2*) and 3 miRNAs (ssc-miR-148a-30, ssc-miR-214-3p and ssc-miR-92b-3p) for qPCR verification. All the analyzed mRNA genes showed a reduced expression in *lean* pigs compared with their *obese* counterparts (**Fig. 2E**) and the *LEP* gene was the most significantly downregulated gene (log_2FC = -1.953; *P*-value = 1.120E-03). This result was in agreement with the strong downregulation observed in differential expression analyses based on RNA-Seq data ((log_2FC = -1.957; *q*-value = 3.443E-03, **Table S9**). With regard to miRNAs, the opposite pattern of expression was observed, with all the three profiled miRNA genes being upregulated in *lean* pigs. Moreover, as reported in **Table S10**, ssc-miR-92b-3p was the miRNA with the most significant upregulation as evidenced in qPCR analyses (*P*-value = 3.57E-02, **Fig. 2F**).

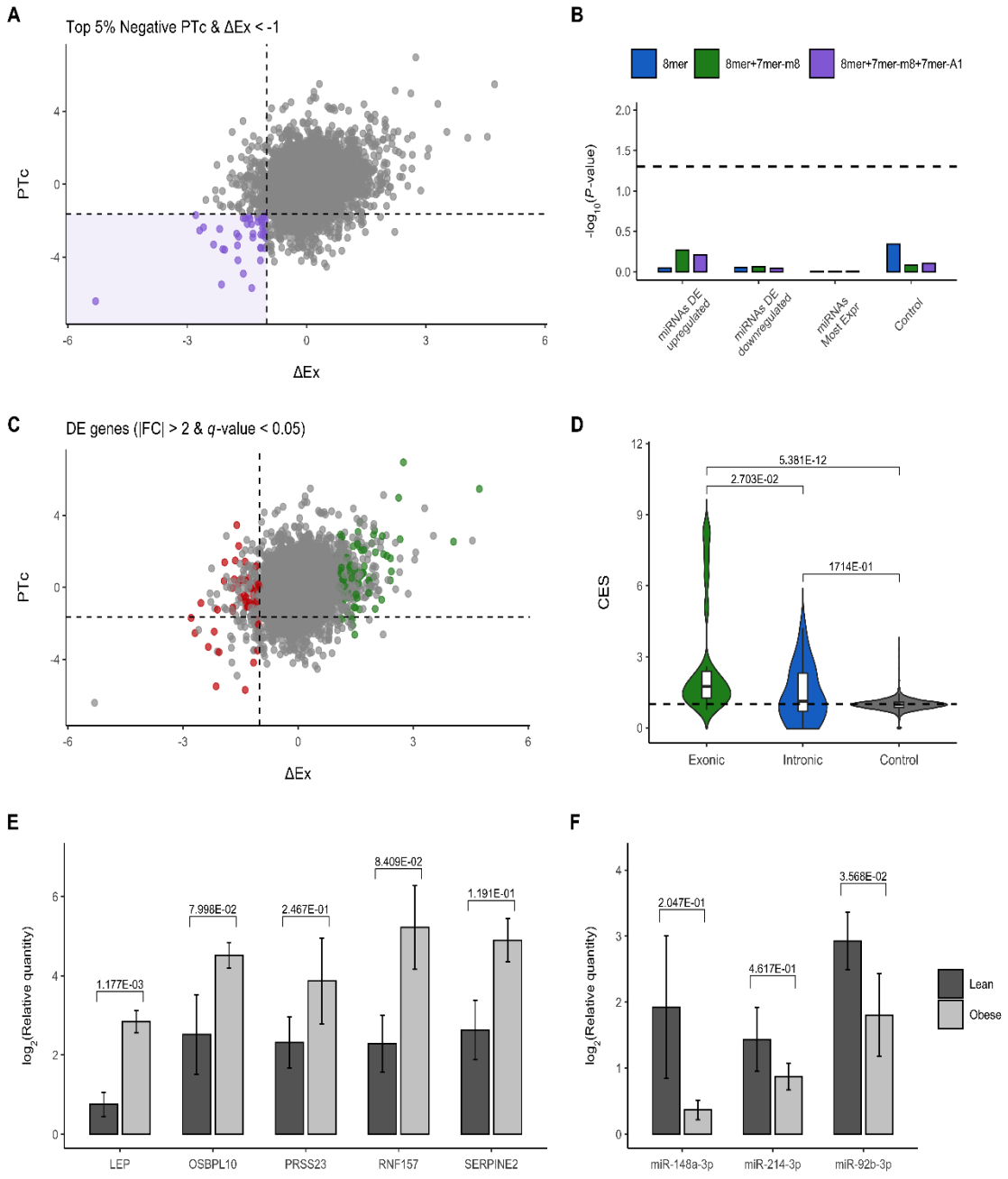

Figure 2: (**A**) Scatterplot depicting mRNA genes with the top 5% negative PTc scores and at least 2-folds ΔEx reduction according to exonic (ΔEx) and PTc (ΔEx – ΔInt) values (in purple) and putatively targeted by upregulated miRNAs (FC > 1.5; *P*-value < 0.01) from adipocyte expression profiles of *lean* (N = 5) and *obese* (N = 5) Duroc-Göttingen minipigs according to their body mass index (BMI). (**B**) Enrichment analyses of the number of mRNA genes with the top 5% negative PTc scores and at least 2-folds ΔEx

503 reduction putatively targeted by DE upregulated miRNAs (FC > 1.5; *q*-value < 0.05), DE
504 downregulated miRNAs (FC < -1.5; *q*-value < 0.05) and the top 5% most highly
505 expressed miRNAs, excluding DE upregulated miRNAs. (**C**) Scatterplot depicting DE
506 upregulated (in green) and downregulated (in red) mRNA genes (|FC| > 2; *q*-value < 0.05)
507 according to exonic (ΔEx) and PTc (ΔEx – ΔInt) values. (**D**) Covariation enrichment
508 scores (CES) for the exonic and intronic fractions of mRNA genes with the top 5%
509 negative PTc scores and at least 2-folds ΔEx reduction, putatively targeted by upregulated
510 miRNAs from adipocyte expression profiles of *lean* (N = 5) and *obese* (N = 5) Duroc-
511 Göttingen minipigs. The control set of CES values were generated by permuted (N =
512 1,000) random sets of exonic and intronic profiles of genes with the same size as those
513 used before (N = 25). Significant differences were assessed using a Mann-Whitney U
514 non-parametric test [48]. (**E**) Barplots depicting qPCR $\log_2$ transformed relative
515 quantities (Rq) for *LEP*, *OSBPL10*, *PRSS23*, *RNF157* and *SERPINE2* mRNA transcripts
516 measured in adipocytes from the retroperitoneal fat of *lean* (N = 5) and *obese* (N = 5)
517 Duroc-Göttingen minipigs. (**F**) Barplots depicting qPCR $\log_2$ transformed relative
518 quantities (Rq) for ssc-miR-148a-3p, ssc-miR-214-3p and ssc-miR-92b-3p miRNA
519 transcripts measured in the isolated adipocytes from the retroperitoneal fat of *lean* (N =
520 5) and *obese* (N = 5) Duroc-Göttingen minipigs.
521
522

523 # 4. Discussion

524 In this study, we undertook the inference of functional miRNA-mRNA interactions using
525 EISA for post-transcriptional signals prioritization, combined with target prediction of
526 upregulated miRNAs, as well as enrichment and covariation analyses.

We observed that the majority of mRNA genes with highly negative PTc scores, i.e., predominantly downregulated at their exonic fractions, also had a coordinated downregulatory effect of their intronic fractions, taken as a proxy of transcriptional repression. This was evidenced by the overall low significance of post-transcriptional signals within the mRNA genes with the top 5% negative PTc scores and reduced ΔEx in both analyzed experimental conditions. Only two genes (*DKK2* and *NAV2*) in *AL-T0* vs *AL-T2* and one gene (*SESN3*) in the *lean* vs *obese* contrasts showed significant PTc scores, revealing that, overall, a coordinated downregulatory effect at both transcriptional and post-transcriptional levels was present, which is in agreement with previous studies using EISA [14,15]. However, it is worth noting that we did not consider the significance of PTc scores as a relevant criterion for prioritizing putative post-transcriptionally downregulated genes, as these will appear as significant when the post-transcriptional activity is the only mechanism modulating the target gene expression profile. Only co-occurring yet opposite transcriptional and post-transcriptional events or single post-transcriptional signals would arise as significant, excluding genes with both coordinated downregulation at the transcriptional and post-transcriptional level.

We decided to use the intronic fraction of expressed mRNAs as a proxy of their transcriptional activity, a source of yet unspliced mRNA transcripts leading to the accumulation of intronic sequences prior to their debranching and degradation by exonucleases. This allows the use of RNA-seq datasets to apply EISA without the need of further experimental procedures, and it can also be applied to investigate transcriptional regulatory signals [15]. Previous reports have also explored the use of specific techniques to capture nascent mRNA transcripts before they are spliced [50–52], and these have been used to account for the transcriptional activity in a similar approach to EISA [53]. Although more advanced methodologies measuring nascent transcription of mRNAs

might provide a better resolution for future experimental designs [54], EISA would still be useful to explore the large amount of available RNA-seq data where additional experiments are no longer possible.

Since the efficacy of miRNA-based regulation on mRNA targets depends on the context of the target site within the 3'-UTR [43], we have described the usefulness of introducing context-based filtering criteria for removing spurious *in silico*-predicted target sites for miRNAs. Using enrichment analyses, we were able to link the downregulated mRNAs at their exonic fractions to upregulated miRNAs that were putatively targeting them and triggering their observed decay in differential expression analyses. The influence of other non-DE highly expressed miRNAs or downregulated miRNAs was discarded by the lack of predicted targeted mRNA genes with high post-transcriptional downregulatory signals for such miRNAs. Overall, the increase in enrichment significance shown for targeted mRNAs with post-transcriptional signals by upregulated miRNAs revealed the ability of context-based filtering criteria to discriminate and remove weak or false positive target sites located within unfavored regions of the 3'-UTR. However, highly efficient target sites such as those of type 8mer, although scarcer than 7mer-m8 sites, might still be functional even at unfavored positions [43,55,56]. This may partially explain the relative lack of 8mer sites found in the top post-transcriptionally regulated mRNA genes in both experimental setups.

Although miRNAs were the major post-transcriptional regulators that we considered in this study, it is important to remark that other additional post-transcriptional modifications and interactions might be responsible for the observed downregulation of mRNAs. For instance, long non-coding RNAs [57], circular RNAs [58,59], RNA methylation [60] or RNA binding proteins [61–63] can all act as post-transcriptional regulators of targeted mRNAs. We further hypothesized that genes showing relevant post-

transcriptional downregulatory effects might be regulated by the same set of significantly upregulated miRNAs, which could induce shared covariation in their expression profiles at the exonic level. On the contrary, their intronic fractions would be mainly unaffected, as introns would have been excised prior to any given miRNA-driven downregulation, if occurring. In this way, an increased gene covariation might be detectable within the sets of commonly targeted mRNA genes with relevant post-transcriptional signals at the exon but not at the intron level, as opposed to covariation events of these set of genes with the rest of DE genes. Our results revealed an increased degree of covariation between genes with high post-transcriptional signals at their exonic fractions, highlighting a putative coordinated downregulation by the set of significantly upregulated miRNAs.

From the analysis of top mRNA genes showing the strongest post-transcriptional downregulatory effects in fasted vs fed gilts, several biological functions putatively regulated by miRNAs were revealed. The *DKK2* gene was the one showing the highest negative PTc score, and its post-transcriptional regulatory signal was also significant, indicating that no additional coordinated transcriptional downregulation was found for this particular gene. Moreover, this gene also showed the strongest covariation difference in its exonic fraction compared with its intronic fraction. This consistent post-transcriptional regulatory effect might be explained by the presence of two miRNA target sites of type 8mer in its 3´-UTR for ssc-miR-421-5p and ssc-miR-30a-3p, two highly DE and upregulated miRNAs. Besides, ssc-miR-30e-3p, a miRNA sharing its seed and regulatory effect with ssc-miR-30a-3p, was also upregulated in fed (*AL-T2*) gilts, which would reinforce the repression of their targeted mRNA transcripts. The *DKK2* gene is a member of the dickkopf family that inhibits the Wnt signaling pathway through its interaction with the LDL-receptor related protein 6 (LRP6). Its repression has been associated with reduced blood-glucose levels and improved glucose uptake [64], as well

602 as with improved adipogenesis [65] and inhibition of aerobic glycolysis [66]. These
603 results agreed with the increased glucose usage and triggered adipogenesis in muscle
604 tissue after nutrient supply. Other additional relevant post-transcriptionally
605 downregulated mRNA genes found by EISA were: (i) pyruvate dehydrogenase kinase 4
606 (*PDK4*), a mitochondrial enzyme that inhibits pyruvate to acetyl-CoA conversion and
607 hinders glucose utilization promoting fatty acids oxidation in energy-deprived cells under
608 fasting conditions [67,68]; (ii) interleukin 18 (*IL18*), involved in controlling energy
609 homeostasis in the muscle by inducing AMP-activated protein kinase (AMPK) [69], a
610 master metabolic regulator that is suppressed upon nutrient influx in cells [70]; (iii)
611 nuclear receptor subfamily 4 group A member 3 (*NR4A3*), which activates both glycolytic
612 and glycogenic factors [71], as well as β-oxidation in muscle cells [72]; (iv) acetylcholine
613 receptor subunit α (*CHRNA1*) of muscle cells, that is linked to the inhibition of nicotine-
614 dependent *STAT3* upregulation [73] that results in protection against insulin resistance in
615 muscle [74]; (v) PBX homeobox 1 (*PBX1*), a regulator of adipocyte differentiation [75];
616 (vi) Tet methylcytosine dioxygenase 2 (*TET2*), linked to glucose-dependent AMPK
617 phosphorylation [76]; and (vii) BTB domain and CNC homolog (*BACH2*), associated
618 with mTOR complex 2 (mTORC2) glucose-dependent activation [77,78] and the
619 repression of forkhead box protein O1 (*FOXO1*) [79] and *PDK4* in a coordinated manner
620 [7,80]. Overall, the highlighted downregulated genes in the muscle of gilts after nutrient
621 supply pointed towards a common regulatory function of miRNAs in modulating glucose
622 uptake and energy homeostasis pathways of the skeletal myocytes.
623 Alternative post-transcriptional regulatory factors other than miRNAs might explain the
624 presence of non-miRNA targets within the top post-transcriptional signals related to
625 regulatory mechanisms not directly involved in energy homeostasis or glucose usage. For
626 instance, three circadian clock-related mRNA genes that showed high post-transcriptional

627 signals were the circadian associated repressor of transcription (*CIART*), period 1 (*PER1*)
628 and salt inducible kinase 1 (*SIK1*), yet the first two were not detected as targets of DE
629 miRNAs. As previously reported for this experimental design [22], the presence of
630 several genes showing abundance differences might reflect a tight feedback interplay
631 among them, where their expression and accumulation are coordinately regulated.
632 Regarding EISA results in RNA-seq profiles of adipocytes from *lean* vs *obese* Duroc-
633 Göttingen minipigs, several of the mRNA genes that showed high post-transcriptional
634 repression are involved in the regulation of lipid metabolism and energy homeostasis.
635 The gene showing the highest post-transcriptional signal was the estrogen related receptor
636 γ (*ESRRG*), which modulates oxidative metabolism and mitochondrial function in
637 adipose tissue and imposes downregulation of adipocyte differentiation when repressed
638 [81]. The second locus highlighted by EISA was sestrin 3 (*SESN3*), an activator of
639 mTORC2 and PI3K/AKT signaling pathway [82] that protects against insulin resistance
640 and promotes lipolysis when inhibited [83]. This gene showed the most significant
641 downregulation in *lean* pigs, and gathered multiple putative binding sites for all the four
642 upregulated miRNAs analyzed. Other genes showing significant post-transcriptional
643 regulation were the following: The sterile α motif domain containing 4A (*SAMD4A*) that
644 has been linked to the inhibition of preadipocyte differentiation and leanness phenotype
645 in knockdown experiments [84,85]. The prostaglandin F2- receptor protein (PTGFR), for
646 which overexpression has been associated with hypertension and obesity risk [86], and
647 its repression appears to improve insulin sensitivity and glucose homeostasis [87]. The
648 expression of serpin E1 and E2 (*SERPINE1*, *SERPINE2*) is linked to obesogenic states
649 and diabetic symptoms [88], while their inhibition improved glucose metabolism [89].
650 The serine protease 23 (PRSS23), which regulates insulin sensitivity and cytokine
651 expression in adipose tissue, and its downregulation confers protective effects against

652 inflammation and reduced fasting glucose level improving insulin resistance [90]. A high
653 expression of ring finger protein 157 (*RNF157*) has been linked to high fatness profiles
654 and increased autophagy in adipose tissue [91]. Silencing of ORP10 protein, encoded by
655 the *OSBLP10* gene, promotes low-density lipoprotein (LDL) synthesis and inhibits
656 lipogenesis [92]. The serum levels of glycosylphosphatidylinositol phospholipase 1
657 (GPLD1) are regulated by insulin and glucose metabolism [93] and linked to the
658 development of insulin resistance and metabolic syndrome [94]. Overexpression of
659 neutrophil cytosolic 2 (*NCF2*), the gene showing the highest increase in covariation at the
660 exonic fraction, was described in obese humans [95]. The repression of RAP1 GTPase
661 activating protein (RAP1GAP) promotes RAP1 activity, which protects against obesity
662 and insulin and glucose resistance [96,97]. Finally, leptin production was also decreased
663 in lean pigs. This key adipokine is mainly produced in adipose tissue [98] and regulates
664 appetite, energy expenditure and body weight [99,100]. In summary, similar to what we
665 found for glucose metabolism and energy homeostasis in the first experimental
666 population, we were also able to describe a set of post-transcriptionally downregulated
667 genes in Duroc-Göttingen minipigs tightly related to adipose tissue metabolism
668 regulation.
669
670

671 # 5. Conclusions

672 In this study we have implemented an exon/intron split analysis of RNA-seq data from
673 skeletal muscle and adipose tissue of pigs in two independent populations. In this way,
674 we were able to identify a set of genes putatively regulated by miRNAs at the post-
675 transcriptional level. Many of these genes were involved in the regulation of energy
676 homeostasis and development of both skeletal muscle and adipose tissues analyzed in the

677 present study, which were in agreement with metabolic modifications in response to
678 nutrient supply and the fatness profile of pigs. Overall, the use of EISA for post-
679 transcriptional signals prioritization combined with target prediction of upregulated
680 miRNAs, as well as enrichment analyses on the set of selected targeted genes and their
681 coordinated covariation, reinforced the usefulness of this approach to infer functional
682 miRNA-mRNA interactions using exonic and intronic fractions of commonly available
683 RNA-seq datasets.

684

685 **Support**

686 The present research work was funded by grants AGL2013-48742-C2-1-R and
687 AGL2013-48742-C2-2-R awarded by the Spanish Ministry of Economy and
688 Competitivity. E. Mármol-Sánchez was funded with a PhD fellowship FPU15/01733
689 awarded by the Spanish Ministry of Education and Culture (MECD). YRC is recipient of
690 a Ramon y Cajal fellowship (RYC2019-027244-I) from the Spanish Ministry of Science
691 and Innovation.

692

693 **Data availability**

694 The RNA-seq and small RNA-seq datasets from skeletal muscle tissue used in the current
695 study are available at the Sequence Read Archive (SRA) database with BioProject codes
696 PRJNA386796 and PRJNA595998, respectively. For the adipose tissue samples, RNA-
697 seq and small RNA-seq datasets are available at PRJNA563583 and PRJNA759240.

698

699 **Conflict of interest**

700 The authors declare no conflict of interest.

701

Acknowledgements

The authors would like to thank the Department of Veterinary Animal Sciences in the Faculty of Health and Medical Sciences of the University of Copenhagen for providing sequencing data and their facilities and resources for qPCR experiments. We also acknowledge Selección Batallé S.A. for providing animal material and the support of the Spanish Ministry of Economy and Competitivity for the Center of Excellence Severo Ochoa 2020–2023 (CEX2019-000902-S) grant awarded to the Centre for Research in Agricultural Genomics (CRAG, Bellaterra, Spain). Thanks also to the CERCA Programme of the Generalitat de Catalunya for their support.

References

[1] N.J. Martinez, A.J.M. Walhout, The interplay between transcription factors and microRNAs in genome-scale regulatory networks, BioEssays. 31 (2009) 435–445. doi:10.1002/bies.200800212.

[2] D.P. Bartel, Metazoan microRNAs, Cell. 173 (2018) 20–51. doi:10.1016/j.cell.2018.03.006.

[3] C.M.J. Mentzel, C. Anthon, M.J. Jacobsen, P. Karlskov-Mortensen, C.S. Bruun, C.B. Jørgensen, J. Gorodkin, S. Cirera, M. Fredholm, Gender and obesity specific microRNA expression in adipose tissue from lean and obese pigs., PLoS One. 10 (2015) e0131650. doi:10.1371/journal.pone.0131650.

[4] H. Han, S. Gu, W. Chu, W. Sun, W. Wei, X. Dang, Y. Tian, K. Liu, J. Chen, miR-17-5p regulates differential expression of *NCOA3* in pig intramuscular and subcutaneous adipose tissue, Lipids. 52 (2017) 939–949. doi:10.1007/s11745-017-4288-4.

[5] W. Wei, B. Li, K. Liu, A. Jiang, C. Dong, C. Jia, J. Chen, H. Liu, W. Wu, Identification of key microRNAs affecting drip loss in porcine longissimus dorsi by RNA-Seq, Gene. 647 (2018) 276–282. doi:10.1016/j.gene.2018.01.005.

[6] S. Xie, X. Li, L. Qian, C. Cai, G. Xiao, S. Jiang, B. Li, T. Gao, W. Cui, L.L. Guan, An integrated analysis of mRNA and miRNA in skeletal muscle from myostatin-edited Meishan pigs, Genome. 62 (2019) 305–315. doi:10.1139/gen-2018-0110.

[7] E. Mármol-Sánchez, Y. Ramayo-Caldas, R. Quintanilla, T.F. Cardoso, R. González-Prendes, J. Tibau, M. Amills, Co-expression network analysis predicts a key role of microRNAs in the adaptation of the porcine skeletal muscle to nutrient supply, J. Anim. Sci. Biotechnol. 11 (2020) 10. doi:10.1186/s40104-019-0412-z.

[8] M.A. Iqbal, A. Ali, F. Hadlich, M. Oster, H. Reyer, N. Trakooljul, V. Sommerfeld, M. Rodehutscord, K. Wimmers, S. Ponsuksili, Dietary phosphorus and calcium in feed affects miRNA profiles and their mRNA targets in jejunum of two strains of laying hens, Sci. Rep. 11 (2021) 13534. doi:10.1038/S41598-021-92932-3.

[9] A. Ali, E. Murani, F. Hadlich, X. Liu, K. Wimmers, S. Ponsuksili, In utero fetal weight in pigs is regulated by microRNAs and their target genes, Genes. 12 (2021) 1264. doi:10.3390/genes12081264.

[10] D. Gaidatzis, L. Burger, M. Florescu, M.B. Stadler, Analysis of intronic and exonic reads in RNA-seq data characterizes transcriptional and post-transcriptional regulation, Nat. Biotechnol. 33 (2015) 722–729. doi:10.1038/nbt.3269.

[11] A. Ameur, A. Zaghlool, J. Halvardson, A. Wetterbom, U. Gyllensten, L. Cavelier, L. Feuk, Total RNA sequencing reveals nascent transcription and widespread co-transcriptional splicing in the human brain., Nat. Struct. Mol. Biol. 18 (2011) 1435–40. doi:10.1038/nsmb.2143.

[12] J.M. Gray, D.A. Harmin, S.A. Boswell, N. Cloonan, T.E. Mullen, J.J. Ling, N.

752 Miller, S. Kuersten, Y.-C. Ma, S.A. McCarroll, S.M. Grimmond, M. Springer,
753 SnapShot-Seq: a method for extracting genome-wide, in vivo mRNA dynamics
754 from a single total RNA sample., PLoS One. 9 (2014) e89673.
755 doi:10.1371/journal.pone.0089673.
756 [13] G.-J. Hendriks, D. Gaidatzis, F. Aeschimann, H. Großhans, Extensive oscillatory
757 gene expression during C. elegans larval development., Mol. Cell. 53 (2014) 380–
758 92. doi:10.1016/j.molcel.2013.12.013.
759
760 [14] J. Cursons, K.A. Pillman, K.G. Scheer, P.A. Gregory, M. Foroutan, S. Hediyeh-
761 Zadeh, J. Toubia, E.J. Crampin, G.J. Goodall, C.P. Bracken, M.J. Davis,
762 Combinatorial targeting by microRNAs co-ordinates post-transcriptional control
763 of EMT, Cell Syst. 7 (2018) 77-91.e7. doi:10.1016/j.cels.2018.05.019.
764 [15] K.A. Pillman, K.G. Scheer, E. Hackett-Jones, K. Saunders, A.G. Bert, J. Toubia,
765 H.J. Whitfield, S. Sapkota, L. Sourdin, H. Pham, T.D. Le, J. Cursons, M.J. Davis,
766 P.A. Gregory, G.J. Goodall, C.P. Bracken, Extensive transcriptional responses are
767 co-ordinated by microRNAs as revealed by Exon–Intron Split Analysis (EISA),
768 Nucleic Acids Res. 47 (2019) 8606-8619. doi:10.1093/nar/gkz664.
769 [16] D. Pérez-Montarelo, A. Fernández, C. Barragán, J.L. Noguera, J.M. Folch, M.C.
770 Rodríguez, C. Óvilo, L. Silió, A.I. Fernández, Transcriptional characterization of
771 porcine leptin and leptin receptor genes, PLoS One. 8 (2013) e66398.
772 doi:10.1371/journal.pone.0066398.
773 [17] C. Ovilo, R. Benítez, A. Fernández, Y. Núñez, M. Ayuso, A.I. Fernández, C.
774 Rodríguez, B. Isabel, A.I. Rey, C. López-Bote, L. Silió, Longissimus dorsi
775 transcriptome analysis of purebred and crossbred Iberian pigs differing in muscle
776 characteristics., BMC Genomics. 15 (2014) 413. doi:10.1186/1471-2164-15-413.

[18] A. Puig-Oliveras, Y. Ramayo-Caldas, J. Corominas, J. Estellé, D. Pérez-Montarelo, N.J. Hudson, J. Casellas, J.M. Folch, M. Ballester, Differences in muscle transcriptome among pigs phenotypically extreme for fatty acid composition., PLoS One. 9 (2014) e99720. doi:10.1371/journal.pone.0099720.

[19] C.M. Pilcher, C.K. Jones, M. Schroyen, A.J. Severin, J.F. Patience, C.K. Tuggle, J.E. Koltes, Transcript profiles in longissimus dorsi muscle and subcutaneous adipose tissue: A comparison of pigs with different postweaning growth rates, J. Anim. Sci. 93 (2015) 2134–2143. doi:10.2527/jas.2014-8593.

[20] M. Ayuso, A. Fernández, Y. Núñez, R. Benítez, B. Isabel, A.I. Fernández, A.I. Rey, A. González-Bulnes, J.F. Medrano, Á. Cánovas, C.J. López-Bote, C. Óvilo, Developmental stage, muscle and genetic type modify muscle transcriptome in pigs: Effects on gene expression and regulatory factors involved in growth and metabolism, PLoS One. 11 (2016) e0167858. doi:10.1371/journal.pone.0167858.

[21] T.F. Cardoso, A. Cánovas, O. Canela-Xandri, R. González-Prendes, M. Amills, R. Quintanilla, RNA-seq based detection of differentially expressed genes in the skeletal muscle of Duroc pigs with distinct lipid profiles, Sci. Rep. 7 (2017) 40005. doi:10.1038/srep40005.

[22] T.F. Cardoso, R. Quintanilla, J. Tibau, M. Gil, E. Mármol-Sánchez, O. González-Rodríguez, R. González-Prendes, M. Amills, Nutrient supply affects the mRNA expression profile of the porcine skeletal muscle, BMC Genomics. 18 (2017) 603. doi:10.1186/s12864-017-3986-x.

[23] J. Horodyska, K. Wimmers, H. Reyer, N. Trakooljul, A.M. Mullen, P.G. Lawlor, R.M. Hamill, RNA-seq of muscle from pigs divergent in feed efficiency and product quality identifies differences in immune response, growth, and macronutrient and connective tissue metabolism, BMC Genomics. 19 (2018) 791.

802 doi:10.1186/s12864-018-5175-y.

803 [24] R. Benítez, N. Trakooljul, Y. Núñez, B. Isabel, E. Murani, E. De Mercado, E.
804 Gómez-Izquierdo, J. García-Casco, C. López-Bote, K. Wimmers, C. Óvilo, Breed,
805 diet, and interaction effects on adipose tissue transcriptome in iberian and duroc
806 pigs fed different energy sources, Genes. 10 (2019) 589.
807 doi:10.3390/genes10080589.

808 [25] M. Ballester, M. Amills, O. González-Rodríguez, T.F. Cardoso, M. Pascual, R.
809 González-Prendes, N. Panella-Riera, I. Díaz, J. Tibau, R. Quintanilla, Role of
810 AMPK signalling pathway during compensatory growth in pigs, BMC Genomics.
811 19 (2018) 682. doi:10.1186/s12864-018-5071-5.

812 [26] L.J.A. Kogelman, H.N. Kadarmideen, T. Mark, P. Karlskov-Mortensen, C.S.
813 Bruun, S. Cirera, M.J. Jacobsen, C.B. Jørgensen, M. Fredholm, An F2 pig resource
814 population as a model for genetic studies of obesity and obesity-related diseases in
815 humans: Design and genetic parameters, Front. Genet. 4 (2013) 29.
816 doi:10.3389/fgene.2013.00029.

817 [27] S.D. Pant, P. Karlskov-Mortensen, M.J. Jacobsen, S. Cirera, L.J.A. Kogelman,
818 C.S. Bruun, T. Mark, C.B. Jørgensen, N. Grarup, E.V.R. Appel, E.A.A. Galjatovic,
819 T. Hansen, O. Pedersen, M. Guerin, T. Huby, P. Lesnik, T.H.E. Meuwissen, H.N.
820 Kadarmideen, M. Fredholm, Comparative analyses of QTLs influencing obesity
821 and metabolic phenotypes in pigs and humans, PLoS One. 10 (2015) e0137356.
822 doi:10.1371/journal.pone.0137356.

823 [28] M.J. Jacobsen, J.H. Havgaard, C. Anthon, C.M.J. Mentzel, S. Cirera, P.M. Krogh,
824 S. Pundhir, P. Karlskov-Mortensen, C.S. Bruun, P. Lesnik, M. Guerin, J. Gorodkin,
825 C.B. Jørgensen, M. Fredholm, R. Barrès, Epigenetic and transcriptomic
826 characterization of pure adipocyte fractions from obese pigs identifies candidate

827 pathways controlling metabolism, Front. Genet. 10 (2019) 1268.
828 doi:10.3389/fgene.2019.01268.
829 [29] P. Decaunes, D. Estève, A. Zakaroff-Girard, C. Sengenès, J. Galitzky, A.
830 Bouloumié, Adipose-derived stromal cells: cytokine expression and immune cell
831 contaminants., Methods Mol. Biol. 702 (2011) 151–161. doi:10.1007/978-1-
832 61737-960-4_12.
833 [30] M. Martin, Cutadapt removes adapter sequences from high-throughput sequencing
834 reads, EMBnet.Journal. 17 (2011) 10. doi:10.14806/ej.17.1.200.
835 [31] A. Warr, N. Affara, B. Aken, H. Beiki, D.M. Bickhart, K. Billis, W. Chow, L.
836 Eory, H.A. Finlayson, P. Flicek, C.G. Girón, D.K. Griffin, R. Hall, G. Hannum, T.
837 Hourlier, K. Howe, D.A. Hume, O. Izuogu, K. Kim, S. Koren, H. Liu, N.
838 Manchanda, F.J. Martin, D.J. Nonneman, R.E. O'Connor, A.M. Phillippy, G.A.
839 Rohrer, B.D. Rosen, L.A. Rund, C.A. Sargent, L.B. Schook, S.G. Schroeder, A.S.
840 Schwartz, B.M. Skinner, R. Talbot, E. Tseng, C.K. Tuggle, M. Watson, T.P.L.
841 Smith, A.L. Archibald, An improved pig reference genome sequence to enable pig
842 genetics and genomics research, Gigascience. 9 (2020) 1–14.
843 doi:10.1093/gigascience/giaa051.
844 [32] D. Kim, J.M. Paggi, C. Park, C. Bennett, S.L. Salzberg, Graph-based genome
845 alignment and genotyping with HISAT2 and HISAT-genotype, Nat. Biotechnol.
846 37 (2019) 907–915. doi:10.1038/s41587-019-0201-4.
847 [33] B. Langmead, C. Trapnell, M. Pop, S.L. Salzberg, Ultrafast and memory-efficient
848 alignment of short DNA sequences to the human genome, Genome Biol. 10 (2009)
849 R25. doi:10.1186/gb-2009-10-3-r25.
850 [34] M. Lawrence, W. Huber, H. Pagès, P. Aboyoun, M. Carlson, R. Gentleman, M.T.
851 Morgan, V.J. Carey, Software for computing and annotating genomic ranges,

PLoS Comput. Biol. 9 (2013) e1003118. doi:10.1371/journal.pcbi.1003118.

[35] Y. Liao, G.K. Smyth, W. Shi, The R package Rsubread is easier, faster, cheaper and better for alignment and quantification of RNA sequencing reads, Nucleic Acids Res. 47 (2019) e47–e47. doi:10.1093/nar/gkz114.

[36] Y. Liao, G.K. Smyth, W. Shi, featureCounts: an efficient general purpose program for assigning sequence reads to genomic features, Bioinformatics. 30 (2014) 923–930. doi:10.1093/bioinformatics/btt656.

[37] M.D. Robinson, D.J. McCarthy, G.K. Smyth, edgeR: a Bioconductor package for differential expression analysis of digital gene expression data., Bioinformatics. 26 (2010) 139–40. doi:10.1093/bioinformatics/btp616.

[38] M.D. Robinson, A. Oshlack, A scaling normalization method for differential expression analysis of RNA-seq data, Genome Biol. 11 (2010) R25. doi:10.1186/gb-2010-11-3-r25.

[39] Y. Benjamini, Y. Hochberg, Controlling the false discovery rate: a practical and powerful approach to multiple testing, J. R. Stat. Soc. Ser. B. 57 (1995) 289–300. doi:10.2307/2346101.

[40] Y. Guo, J. Liu, S.J. Elfenbein, Y. Ma, M. Zhong, C. Qiu, Y. Ding, J. Lu, Characterization of the mammalian miRNA turnover landscape, Nucleic Acids Res. 43 (2015) 2326–2341. doi:10.1093/nar/gkv057

[41] A. Kozomara, M. Birgaoanu, S. Griffiths-Jones, MiRBase: From microRNA sequences to function, Nucleic Acids Res. 47 (2019) D155–D162. doi:10.1093/nar/gky1141.

[42] A. Marco, SeedVicious: Analysis of microRNA target and near-target sites, PLoS One. 13 (2018) e0195532. doi:10.1371/journal.pone.0195532.

[43] A. Grimson, K.K.H. Farh, W.K. Johnston, P. Garrett-Engele, L.P. Lim, D.P.

877 Bartel, MicroRNA targeting specificity in mammals: determinants beyond seed
878 pairing, Mol. Cell. 27 (2007) 91–105. doi:10.1016/j.molcel.2007.06.017.
879 [44] R.C. Friedman, K.K.H. Farh, C.B. Burge, D.P. Bartel, Most mammalian mRNAs
880 are conserved targets of microRNAs, Genome Res. 19 (2009) 92–105.
881 doi:10.1101/gr.082701.108.
882 [45] A. Reverter, E.K.F. Chan, Combining partial correlation and an information theory
883 approach to the reversed engineering of gene co-expression networks,
884 Bioinformatics. 24 (2008) 2491–2497. doi:10.1093/bioinformatics/btn482.
885 [46] N.S. Watson-Haigh, H.N. Kadarmideen, A. Reverter, PCIT: an R package for
886 weighted gene co-expression networks based on partial correlation and
887 information theory approaches, Bioinformatics. 26 (2010) 411–413.
888 doi:10.1093/bioinformatics/btp674.
889 [47] M. Tarbier, S.D. Mackowiak, J. Frade, S. Catuara-Solarz, I. Biryukova, E. Gelali,
890 D.B. Menéndez, L. Zapata, S. Ossowski, M. Bienko, C.J. Gallant, M.R.
891 Friedländer, Nuclear gene proximity and protein interactions shape transcript
892 covariations in mammalian single cells, Nat. Commun. 11 (2020) 5445.
893 doi:10.1038/s41467-020-19011-5.
894 [48] H.B. Mann, D.R. Whitney, On a test of whether one of two random variables is
895 stochastically larger than the other, Ann. Math. Stat. 18 (1947) 50–60.
896 doi:10.1214/aoms/1177730491.
897 [49] A.B. Nygard, C.B. Jørgensen, S. Cirera, M. Fredholm, Selection of reference genes
898 for gene expression studies in pig tissues using SYBR green qPCR, BMC Mol.
899 Biol. 8 (2007) 67. doi:10.1186/1471-2199-8-67.
900 [50] L.J. Core, J.J. Waterfall, J.T. Lis, Nascent RNA sequencing reveals widespread
901 pausing and divergent initiation at human promoters, Science. 322 (2008) 1845–

902 1848. doi:10.1126/science.1162228.

903 [51] D.B. Mahat, H. Kwak, G.T. Booth, I.H. Jonkers, C.G. Danko, R.K. Patel, C.T.
904 Waters, K. Munson, L.J. Core, J.T. Lis, Base-pair resolution genome-wide
905 mapping of active RNA polymerasesusing precision nuclear run-on (PRO-seq),
906 Nat. Protoc. 11 (2016) 1455. doi:10.1038/nprot.2016.086.

907 [52] A. Blumberg, Y. Zhao, Y.-F. Huang, N. Dukler, E.J. Rice, A.G. Chivu, K.
908 Krumholz, C.G. Danko, A. Siepel, Characterizing RNA stability genome-wide
909 through combined analysis of PRO-seq and RNA-seq data, BMC Biol. 19 (2021)
910 30. doi:10.1186/s12915-021-00949-x.

911 [53] R.K. Patel, J.D. West, Y. Jiang, E.A. Fogarty, A. Grimson, Robust partitioning of
912 microRNA targets from downstream regulatory changes, Nucleic Acids Res. 48
913 (2020) 9724–9746. doi:10.1093/nar/gkaa687.

914 [54] E.M. Wissink, A. Vihervaara, N.D. Tippens, J.T. Lis, Nascent RNA analyses:
915 tracking transcription and its regulation, Nat. Rev. Gen. 20 (2019) 705-723.
916 doi:10.1038/s41576-019-0159-6.

917 [55] R. Denzler, S.E. McGeary, A.C. Title, V. Agarwal, D.P. Bartel, M. Stoffel, Impact
918 of microRNA levels, target-site complementarity, and cooperativity on competing
919 endogenous RNA-regulated gene expression, Mol. Cell. 64 (2016) 565-579.
920 doi:10.1016/j.molcel.2016.09.027.

921 [56] S.E. McGeary, K.S. Lin, C.Y. Shi, T.M. Pham, N. Bisaria, G.M. Kelley, D.P.
922 Bartel, The biochemical basis of microRNA targeting efficacy, Science. 366
923 (2019) eaav1741. doi:10.1126/science.aav1741.

924 [57] R.Z. He, D.X. Luo, Y.Y. Mo, Emerging roles of lncRNAs in the post-
925 transcriptional regulation in cancer, Genes Dis. 6 (2019) 6–15.
926 doi:10.1016/j.gendis.2019.01.003.

927 [58] S. Memczak, M. Jens, A. Elefsinioti, F. Torti, J. Krueger, A. Rybak, L. Maier, S.D.
928 Mackowiak, L.H. Gregersen, M. Munschauer, A. Loewer, U. Ziebold, M.
929 Lanthaler, C. Kocks, F. le Noble, N. Rajewsky, Circular RNAs are a large class of
930 animal RNAs with regulatory potency, Nature. 495 (2013) 333–338.
931 doi:10.1038/nature11928.
932 [59] P.G. Maass, P. Glažar, S. Memczak, G. Dittmar, I. Hollfinger, L. Schreyer, A.V.
933 Sauer, O. Toka, A. Aiuti, F.C. Luft, N. Rajewsky, A map of human circular RNAs
934 in clinically relevant tissues, J. Mol. Med. (Berl). 95 (2017) 1179–1189.
935 doi:10.1007/S00109-017-1582-9.
936 [60] B.S. Zhao, I.A. Roundtree, C. He, Post-transcriptional gene regulation by mRNA
937 modifications, Nat. Rev. Mol. Cell Biol. 18 (2017) 31. doi:10.1038/nrm.2016.132.
938 [61] T. Glisovic, J.L. Bachorik, J. Yong, G. Dreyfuss, RNA-binding proteins and post-
939 transcriptional gene regulation, FEBS Lett. 582 (2008) 1977–1986.
940 doi:10.1016/j.febslet.2008.03.004.
941 [62] M.W. Hentze, A. Castello, T. Schwarzl, T. Preiss, A brave new world of RNA-
942 binding proteins, Nat. Rev. Mol. Cell Biol. 19 (2018) 327–341.
943 doi:10.1038/nrm.2017.130.
944 [63] A. Velázquez-Cruz, B. Baños-Jaime, A. Díaz-Quintana, M.A.D. la Rosa, I. Díaz-
945 Moreno, Post-translational control of RNA-binding proteins and disease-related
946 dysregulation, Front. Mol. Biosci. 8 (2021) 658852.
947 doi:10.3389/fmolb.2021.658852.
948 [64] X. Li, J. Shan, W. Chang, I. Kim, J. Bao, H.-J. Lee, X. Zhang, V.T. Samuel, G.I.
949 Shulman, D. Liu, J.J. Zheng, D. Wu, Chemical and genetic evidence for the
950 involvement of Wnt antagonist Dickkopf2 in regulation of glucose metabolism,
951 Proc. Natl. Acad. Sci. 109 (2012) 11402–11407. doi:10.1073/pnas.1205015109.

952 [65] J. Yang, B. yin Shi, Dickkopf (Dkk)-2 is a beige fat-enriched adipokine to regulate
953 adipogenesis, Biochem. Biophys. Res. Commun. 548 (2021) 211–216.
954 doi:10.1016/j.bbrc.2021.02.068.
955 [66] F. Deng, R. Zhou, C. Lin, S. Yang, H. Wang, W. Li, K. Zheng, W. Lin, X. Li, X.
956 Yao, M. Pan, L. Zhao, Tumor-secreted dickkopf2 accelerates aerobic glycolysis
957 and promotes angiogenesis in colorectal cancer, Theranostics. 9 (2019) 1001-1014.
958 doi:10.7150/thno.30056.
959 [67] J.Y. Jeong, N.H. Jeoung, K.-G. Park, I.-K. Lee, Transcriptional regulation of
960 pyruvate dehydrogenase kinase, Diabetes Metab. J. 36 (2012) 328–35.
961 doi:10.4093/dmj.2012.36.5.328.
962 [68] S. Zhang, M.W. Hulver, R.P. McMillan, M.A. Cline, E.R. Gilbert, The pivotal role
963 of pyruvate dehydrogenase kinases in metabolic flexibility, Nutr. Metab. 11 (2014)
964 10. doi:10.1186/1743-7075-11-10.
965 [69] B. Lindegaard, V.B. Mathews, C. Brandt, P. Hojman, T.L. Allen, E. Estevez, M.J.
966 Watt, C.R. Bruce, O.H. Mortensen, S. Syberg, C. Rudnika, J. Abildgaard, H.
967 Pilegaard, J. Hidalgo, S. Ditlevsen, T.J. Alsted, A.N. Madsen, B.K. Pedersen, M.A.
968 Febbraio, Interleukin-18 activates skeletal muscle AMPK and reduces weight gain
969 and insulin resistance in mice, Diabetes. 62 (2013) 3064–3074. doi:10.2337/DB12-
970 1095.
971 [70] P. Jiang, L. Ren, L. Zhi, Z. Yu, F. Lv, F. Xu, W. Peng, X. Bai, K. Cheng, L, Quang,
972 X. Zhang, X. Wang, Y. Zhang, D. Yang, X. Hu, R.P. Xiao, Negative regulation of
973 AMPK signaling by high glucose via E3 ubiquitin ligase MG53, Mol. Cell. 81
974 (2021) 629-637.e5. doi:10.1016/j.molcel.2020.12.008.
975 [71] C. Zhang, B. Zhang, X. Zhang, G. Sun, X. Sun, Targeting orphan nuclear receptors
976 NR4As for energy homeostasis and diabetes, Front. Pharmacol. 11 (2020) 587457.

977 doi:10.3389/fphar.2020.587457.

978 [72] M.A. Pearen, J.M. Goode, R.L. Fitzsimmons, N.A. Eriksson, G.P. Thomas, G.J.
979 Cowin, S.C. Wang, Z.K. Tuong, G.E. Muscat, Transgenic muscle-specific Nor-1
980 expression regulates multiple pathways that effect adiposity, metabolism, and
981 endurance, Mol. Endocrinol. 27 (2013) 1897–1917. doi:10.1210/me.2013-1205.

982 [73] S. Xu, H. Ni, H. Chen, Q. Dai, The interaction between STAT3 and nAChRα1
983 interferes with nicotine-induced atherosclerosis via Akt/mTOR signaling cascade,
984 Aging. 11 (2019) 8120–8138. doi:10.18632/aging.102296.

985 [74] L. Zhang, Z. Chen, Y. Wang, D.J. Tweardy, W.E. Mitch, Stat3 activation induces
986 insulin resistance via a muscle-specific E3 ubiquitin ligase Fbxo40, Am. J. Physiol.
987 Endocrinol. Metab. 318 (2020) E625–E635. doi:10.1152/ajpendo.00480.2019.

988 [75] M.C. Monteiro, M. Sanyal, M.L. Cleary, C. Sengenès, A. Bouloumié, C. Dani, N.
989 Billon, PBX1: a novel stage-specific regulator of adipocyte development, Stem
990 Cells. 29 (2011) 1837–1848. doi:10.1002/stem.737.

991 [76] D. Wu, D. Hu, H. Chen, G. Shi, I.S. Fetahu, F. Wu, K. Rabidou, R. Fang, L. Tan,
992 S. Xu, H. Liu, C. Argueta, L. Zhang, F. Mao, G. Yan, J. Chen, Z. Dong, R. Lv, Y.
993 Xu, M. Wang, Y. Ye, S. Zhang, D. Duquette, S. Geng, C. Yin, C.G. Lian, G.F.
994 Murphy, G.K. Adler, R. Garg, L. Lynch, P. Yang, Y. Li, F. Lan, J. Fan, Y. Shi,
995 Y.G. Shi, Glucose-regulated phosphorylation of TET2 by AMPK reveals a
996 pathway linking diabetes to cancer, Nature. 559 (2018) 637–641.
997 doi:10.1038/s41586-018-0350-5.

998 [77] T. Tamahara, K. Ochiai, A. Muto, Y. Kato, N. Sax, M. Matsumoto, T. Koseki, K.
999 Igarashi, The mTOR-Bach2 cascade controls cell cycle and class switch
1000 recombination during B cell differentiation, Mol. Cell. Biol. 37 (2017) e00418-17.
1001 doi:10.1128/mcb.00418-17.

[78] G. Leprivier, B. Rotblat, How does mTOR sense glucose starvation? AMPK is the usual suspect, Cell Death Discov. 6 (2020) 27. doi:10.1038/S41420-020-0260-9.

[79] A. Itoh-Nakadai, M. Matsumoto, H. Kato, J. Sasaki, Y. Uehara, Y. Sato, R. Ebina-Shibuya, M. Morooka, R. Funayama, K. Nakayama, K. Ochiai, A. Muto, K. Igarashi, A Bach2-Cebp gene regulatory network for the commitment of multipotent hematopoietic progenitors, Cell Rep. 18 (2017) 2401–2414. doi:10.1016/j.celrep.2017.02.029.

[80] K. Gopal, B. Saleme, R. Al Batran, H. Aburasayn, A. Eshreif, K.L. Ho, W.K. Ma, M. Almutairi, F. Eaton, M. Gandhi, E.A. Park, G. Sutendra, J.R. Ussher, FoxO1 regulates myocardial glucose oxidation rates via transcriptional control of pyruvate dehydrogenase kinase 4 expression, Am. J. Physiol. Circ. Physiol. 313 (2017) H479–H490. doi:10.1152/ajpheart.00191.2017.

[81] M. Kubo, N. Ijichi, K. Ikeda, K. Horie-Inoue, S. Takeda, S. Inoue, Modulation of adipogenesis-related gene expression by estrogen-related receptor γ during adipocytic differentiation, Biochim. Biophys. Acta - Gene Regul. Mech. 1789 (2009) 71–77. doi:10.1016/j.bbgram.2008.08.012.

[82] X. Huang, G. Liu, J. Guo, Z. Su, The PI3K/AKT pathway in obesity and type 2 diabetes, Int. J. Biol. Sci. 14 (2018) 1483. doi:10.7150/ijbs.27173.

[83] R. Tao, X. Xiong, S. Liangpunsakul, X.C. Dong, Sestrin 3 protein enhances hepatic insulin sensitivity by direct activation of the mTORC2-Akt signaling, Diabetes. 64 (2015) 1211–1223. doi:10.2337/db14-0539.

[84] Z. Chen, W. Holland, J.M. Shelton, A. Ali, X. Zhan, S. Won, W. Tomisato, C. Liu, X. Li, E.M.Y. Moresco, B. Beutler, Mutation of mouse *Samd4* causes leanness, myopathy, uncoupled mitochondrial respiration, and dysregulated mTORC1 signaling, Proc. Natl. Acad. Sci. 111 (2014) 7367–7372.

doi:10.1073/pnas.1406511111.

[85] Y. Liu, H. Liu, Y. Li, R. Mao, H. Yang, Y. Zhang, Y. Zhang, P. Guo, D. Zhan, T. Zhang, Circular RNA *SAMD4A* controls adipogenesis in obesity through the miR-138-5p/EZH2 axis, Theranostics. 10 (2020) 4705–4719. doi:10.7150/thno.42417.

[86] B. Xiao, S.M. Gu, M.J. Li, J. Li, B. Tao, Y. Wang, Y. Wang, S. Zuo, Y. Shen, Y. Yu, D. Chen, G. Chen, D. Kong, J. Tang, Q. Liu, D.R. Cheng, Y. Liu, S. Alberti, M. Dovizio, R. Landolfi, L. Mucci, P.-Z. Miao, P. Gao, D.-L. Zhu, J. Wang, B. Li, P. Patrignani, Y. Yu, Rare SNP rs12731181 in the miR-590-3p target site of the Prostaglandin F2α receptor gene confers risk for essential hypertension in the Han Chinese population, Arterioscler. Thromb. Vasc. Biol. 35 (2015) 1687–1695. doi:10.1161/atvbaha.115.305445.

[87] Y. Wang, S. Yan, B. Xiao, S. Zuo, Q. Zhang, G. Chen, Y. Yu, D. Chen, Q. Liu, Y. Liu, Y. Shen, Y. Yu, Prostaglandin F 2α facilitates hepatic glucose production through CaMKIIγ/p38/FOXO1 signaling pathway in fasting and obesity, Diabetes. 67 (2018) 1748–1760. doi:10.2337/db17-1521.

[88] P. Kaur, M.D. Reis, G.R. Couchman, S.N. Forjuoh, J.F. Greene, Jr, A. Asea, SERPINE 1 links obesity and diabetes: a pilot study, J. Proteomics Bioinform. 3 (2010) 191. doi:10.4172/jpb.1000139.

[89] G.M. Coudriet, J. Stoops, A.V. Orr, B. Bhushan, K. Koral, S. Lee, D.M. Previte, H.H. Dong, G.K. Michalopoulos, W.M. Mars, J.D. Piganelli, A Noncanonical role for plasminogen activator inhibitor type 1 in obesity-induced diabetes, Am. J. Pathol. 189 (2019) 1413–1422. doi:10.1016/j.ajpath.2019.04.004.

[90] C.-S. Kuo, J.-S. Chen, L.-Y. Lin, G.W. Schmid-Schönbein, S. Chien, P.-H. Huang, J.-W. Chen, S.-J. Lin, Inhibition of serine protease activity protects against high fat diet-induced inflammation and insulin resistance, Sci. Reports. 10 (2020) 1–11.

doi:10.1038/s41598-020-58361-4.

[91] J. Kosacka, M. Nowicki, S. Paeschke, P. Baum, M. Blüher, N. Klö ting, Up-regulated autophagy: as a protective factor in adipose tissue of WOKW rats with metabolic syndrome, Diabetol. Metab. Syndr. 10 (2018) 13. doi:10.1186/S13098-018-0317-6.

[92] J. Perttilä, K. Merikanto, J. Naukkarinen, I. Surakka, N.W. Martin, K. Tanhuanpää, V. Grimard, M.-R. Taskinen, C. Thiele, V. Salomaa, A. Jula, M. Perola, I. Virtanen, L. Peltonen, V.M. Olkkonen, OSBPL10, a novel candidate gene for high triglyceride trait in dyslipidemic Finnish subjects, regulates cellular lipid metabolism, J. Mol. Med. 2009 878. 87 (2009) 825–835. doi:10.1007/S00109-009-0490-Z.

[93] R.F. Bowen, N.S. Raikwar, L.K. Olson, M.A. Deeg, Glucose and insulin regulate glycosylphosphatidylinositol-specific phospholipase D expression in islet beta cells, Metabolism. 50 (2001) 1489–1492. doi:10.1053/meta.2001.28087.

[94] S. Ussar, O. Bezy, M. Blüher, C.R. Kahn, Glypican-4 enhances insulin signaling via interaction with the insulin receptor and serves as a novel adipokine, Diabetes. 61 (2012) 2289–2298. doi:10.2337/db11-1395.

[95] J. Xu, X. Bao, Z. Peng, L. Wang, L. Du, W. Niu, Y. Sun, Comprehensive analysis of genome-wide DNA methylation across human polycystic ovary syndrome ovary granulosa cell, Oncotarget. 7 (2016) 27899. doi:10.18632/oncotarget.8544.

[96] F. Yeung, C.M. Ramírez, P.A. Mateos-Gomez, A. Pinzaro, G. Ceccarini, S. Kabir, C. Fernández-Hernando, A. Sfeir, Nontelomeric role for Rap1 in regulating metabolism and protecting against obesity, Cell Rep. 3 (2013) 1847–1856. doi:10.1016/j.celrep.2013.05.032.

[97] P. Martínez, G. Gómez-López, F. García, E. Mercken, S. Mitchell, J.M. Flores, R.

de Cabo, M.A. Blasco, RAP1 protects from obesity through its extratelomeric role regulating gene expression, Cell Rep. 3 (2013) 2059–2074. doi:10.1016/j.celrep.2013.05.030.

[98] W. Yang, T. Kelly, J. He, Genetic epidemiology of obesity, Epidemiol. Rev. 29 (2007) 49–61. doi:10.1093/epirev/mxm004.

[99] Y. Zhou, L. Rui, Leptin signaling and leptin resistance, Front. Med. 7 (2013) 207–222. doi:10.1007/s11684-013-0263-5.

[100] A.G. Izquierdo, A.B. Crujeiras, F.F. Casanueva, M.C. Carreira, Leptin, obesity, and leptin resistance: where are we 25 years later?, Nutrients. 11 (2019) 2704. doi:10.3390/nu11112704.

Supplementary Tables

Table S1: Phenotype values for selected Duroc-Göttingen minipigs from the F2-UNIK resource population according to their body mass indexes.

Table S2: Primers for qPCR validation of selected mRNA and miRNA genes according to EISA results in the F2-UNIK Duroc-Göttingen minipig population comparing *lean* (N = 5) and *obese* (N = 5) individuals.

Table S3: Raw Cq values from qPCR analyses after efficiency correction measuring adipocyte expression profiles of selected mRNAs and miRNAs from *lean* (N = 5) and *obese* (N = 5) Duroc-Göttingen minipigs.

Table S4: Genes detected by *edgeR* tool as differentially expressed when comparing *gluteus medius* expression profiles of fasted *AL-T0* (N = 11) and fed *AL-T2* (N = 12) Duroc gilts.

Table S5: microRNAs detected by *edgeR* tool as differentially expressed when comparing *gluteus medius* expression profiles of fasted *AL-T0* (N = 11) and fed *AL-T2* (N = 12) Duroc gilts.

Table S6: EISA results for post-transcriptional signals (PTc) detected in *gluteus medius* skeletal muscle expression profiles of fasted (*AL-T0*, N = 11) and fed (*AL-T2*, N = 12) Duroc gilts.

Table S7: Binding sites for differentially upregulated miRNAs found in mRNA genes with the top 5% negative PT_c scores and at least 2-folds reduction in the exonic fraction (ΔEx) of *gluteus medius* skeletal muscle expression profiles from fasting (*AL-T0*, N = 11) and fed (*AL-T2*, N = 12) Duroc gilts.

Table S8: Covariation enrichment scores (CES) for the exonic and intronic fractions of mRNA genes with the top 5% negative post-transcriptional signals (PTc) and at least 2-folds reduction in their exonic (ΔEx) fraction, that were putatively targeted by DE upregulated miRNAs from *gluteus medius* skeletal muscle expression profiles *AL-T0 vs AL-T2* Duroc gilts.

Table S9: Genes detected by *edgeR* tool as differentially expressed when comparing adipocyte expression profiles from *lean* (N = 5) and *obese* (N = 5) Duroc-Göttingen minipigs according to their body mass index.

Table S10: microRNA genes detected by *edgeR* tool as differentially expressed when comparing adipocyte expression profiles from *lean* (N = 5) and *obese* (N = 5) Duroc-Göttingen minipigs according to their body mass index.

Table S11: mRNA genes with the top 5% post-transcriptional signals (PTc) and at least 2-fold exonic fraction (ΔEx) reduction (equivalent to -1 in the log2 scale) from adipocyte expression profiles of *lean* (N = 5) and *obese* (N = 5) Duroc-Göttingen minipigs according to their body mass index.

Table S12: EISA results for post-transcriptional signals (PTc) detected in adipocyte expression profiles of *lean* (N = 5) and *obese* (N = 5) Duroc-Göttingen minipigs according to their body mass index.

Table S13: Binding sites for differentially upregulated miRNAs found in mRNA genes with the top 5% negative PTc scores and at least 2-folds reduction in the exonic fraction (ΔEx) of adipocyte expression profiles from *lean* (N = 5) and *obese* (N = 5) Duroc-Göttingen minipigs according to their body mass index.

Table S14: Covariation enrichment scores (CES) for the exonic and intronic fractions of mRNA genes with the top 5% negative post-transcriptional signals (PTc) and at least 2-folds reduction in their exonic (ΔEx) fraction, that were putatively targeted by DE

upregulated miRNAs from adipocyte expression profiles of *lean* vs *obese* Duroc-Göttingen minipigs.

Supplementary Figures

Figure S1: Diagram depicting the consecutive steps implemented for studying miRNA-driven post-transcriptional regulatory signals applying the EISA approach and additional enrichment and covariation analyses.

Figure S2: Scatterplots depicting the exonic (ΔEx) and intronic (ΔInt) fractions from *gluteus medius* skeletal muscle expression profiles of fasting (*AL-T0*, N = 11) and fed (*AL-T2*, N = 12) Duroc gilts. (**A**) mRNA genes with the top 5% post-transcriptional (PTc) negative scores and at least 2-folds reduced exonic (ΔEx) fractions (equivalent to -1 in the $\log_2$ scale), suggestive of miRNA-driven post-transcriptional regulation. (**B**) mRNA genes differentially expressed showing upregulation (FC > 2; *q*-value < 0.05, in green) and downregulation (FC < -2, *q*-value < 0.05, in red) in fed (*AL-T2*, N = 12) Duroc gilts with respect to their fasted (*AL-T0*, N = 11) counterparts.

Figure S3: Enrichment analyses of the number of genes with the (**A**) top 1% and (**B**) top 5% negative PTc scores and at least 2-fold reduced exonic fractions (ΔEx) putatively targeted by upregulated miRNAs (FC > 1.5; *q*-value < 0.05) from *gluteus medius* skeletal muscle expression profiles of fasting (*AL-T0*, N = 11) and fed (*AL-T2*, N = 12) Duroc gilts. Results show the change in enrichment significance when incorporating context-based pruning of miRNA binding sites of type 8mer, 7mer-m8 and 7mer-A1. R: Raw enrichment analyses without any additional context-based pruning. AU: Enrichment

analyses removing miRNA binding sites without AU-rich flanking sequences (30 nts upstream and downstream). M: Enrichment analyses removing miRNA binding sites located in the middle of the 3'-UTR sequence (45-55%). E: Enrichment analyses removing miRNA binding sites located too close (< 15 nts) to the beginning or the end of the 3'-UTR sequences. The black dashed line represents a *P*-value = 0.05.